
Alpha-RTL: Test-Time Training for RTL Hardware Optimization

Peilong Zhou^{1,2,3}, Zhirong Chen^{1,2}, Cangyuan Li^{1,2}, Haoyu Gao^{1,2,3},
Kaiyan Chang^{1,2}, Ziming Qu^{1,2}, Ying Wang^{1,2}

¹SKLP, Institute of Computing Technology, Chinese Academy of Sciences

²University of the Chinese Academy of Sciences ³School of Advanced Interdisciplinary Sciences

Correspondence: wangying2009@ict.ac.cn

Abstract

Large language models (LLMs) have shown increasing promise in generating functionally correct register-transfer-level (RTL) hardware designs. Recent LLM-for-RTL systems further improve this ability through Verilog-domain distillation, RLVR with automated testbenches, or EDA-integrated reinforcement learning with syntax, simulation, and PPA rewards. However, these methods primarily train a general RTL generator before deployment, while test-time approaches typically search with a frozen policy. We instead perform reinforcement learning at test time, allowing the LLM policy to adapt to executable EDA feedback from the specific RTL optimization problem. This setting is challenging because candidate designs must pass sparse discrete validity gates—syntax checking and simulation—before receiving meaningful synthesis-derived feedback on area, timing, or power. We propose **TTT-RTL**, to our knowledge the first *per-design* test-time training framework that closes the loop between an LLM policy and an EDA pipeline for RTL optimization. TTT-RTL samples candidate implementations, verifies them through syntax checking and simulation, scores valid designs using synthesis-derived PPA product, reuses high-reward variants through a PUCT-indexed design-state pool, and updates the policy with an entropic policy-gradient objective. To stabilize policy updates under sparse or plateaued reward groups, we introduce an adaptive KL-budget controller that adjusts the entropy constraint using reference KL, effective sample size, constant-reward fraction, and beta-search saturation. On RTLLM v2.0 under Nangate 45 nm, TTT-RTL reduces the geometric-mean PPA product by 65.1% over the reference, outperforming the strongest published frozen-policy agent baseline under the same reference-normalized metric at 26.1%. On an industrial XuanTie C910 FPU leading-zero-anticipation unit under Sky130, TTT-RTL achieves a 59.4% ADP reduction over the original implementation, and ablations show that policy adaptation, state reuse, and KL-budget control each contribute to the gain. These results suggest that test-time training with executable EDA feedback can move LLM-based RTL generation beyond functional correctness toward physically optimized hardware.

1 Introduction

Hardware design is a laborious process whose quality is ultimately judged by physical metrics: area, clock frequency, and power consumption. Modern EDA flows translate a register-transfer-level (RTL) description written in Verilog or VHDL into a physical circuit; the resulting *PPA product* (Area×Delay×Power, the joint figure of merit used by RTLLM v2.0 reports) depends not only on

the logical correctness of the code but on fine-grained micro-architectural choices— pipeline depth, operator scheduling, signal encoding—that are difficult to predict without running synthesis.

Recent work has shown that LLMs can generate functionally correct RTL code [Liu et al., 2023b,c, Blocklove et al., 2023]. These models learn to imitate high-quality Verilog from training corpora, and when prompted with a hardware specification they can produce designs that pass functional simulation. However, functional correctness is a necessary but insufficient condition for hardware quality. A multiplier that passes all testbench cases may still be 30% larger or 30% slower than an optimized reference implementation. Because physical synthesis metrics are computed by EDA tools at evaluation time—not during LLM training—existing models cannot learn to minimize the PPA product.

Existing approaches to optimize RTL fall into two families, each capturing only half of what is needed. **Frozen-LLM search agents**—EvoLVE [Hsin et al., 2026], VeriAgent [Wang et al., 2026], and the current SOTA REvolution [Min et al., 2025]—drive an LLM through evolutionary or reflective loops with synthesis feedback, but the weights never update: search quality is bounded by the unchanged base policy, and the design knowledge accumulated from EDA tools is discarded the moment the run ends. **Training-time RL methods**—ChipSeek [Chen et al., 2025] and EARL [Shi et al., 2025]—do learn from synthesis signals, but they ship a single amortized policy evaluated under Pass@ k : each candidate is an independent single-shot generation, with no mechanism to feed EDA results from one attempt back into the next on the same design.

We argue the missing regime is to *fuse search into training at test time*: given one design and its reference, run a multi-round search whose every rollout’s EDA feedback updates the model *online for that problem*, so the policy itself deepens as the search progresses. Concretely, we treat Verilog candidates as nodes in a PUCT tree whose every expansion is scored by a three-stage EDA pipeline (syntax \rightarrow simulation \rightarrow synthesis), and we feed that dense physical reward back into online policy-gradient updates on the same design. The result is a closed loop in which exploration and training co-evolve under EDA-grounded feedback, rather than search being grafted on top of a frozen policy. On RTLLM v2.0 this regime substantially outperforms the strongest published agent baseline on PPA-product reduction, and on a XuanTie C910 industrial floating-point unit it improves over well-tuned production RTL—we quantify both below.

Contributions.

1. We formulate per-design RTL optimization as a test-time training problem, fusing PUCT-guided search into online policy updates driven by EDA feedback.
2. We propose **TTT-RTL**, instantiating this regime with a Verilog state pool, EDA-feedback prompting, an entropic advantage estimator, and a three-stage syntax/simulation/ synthesis reward, built on ver1 [Sheng et al., 2024].
3. On **RTLLM v2.0** TTT-RTL covers 48/49 designs and cuts the PPA product by a geometric-mean of 65.1% vs. 26.1% for the strongest published agent baseline (REvolution); on a **XuanTie C910** industrial LZA unit it improves over well-tuned production RTL by 59.4% ADP at seed 42, with single-seed component ablations isolating the contribution of the PUCT pool and the entropic estimator.

2 Related Work

2.1 Test-time training and RL with verifiable rewards

Test-time training (TTT) [Sun et al., 2020] updates model parameters at inference time using an auxiliary self-supervised objective constructed from the test input. Yuksekogonul et al. [2026] extended TTT to discrete reasoning via **PUCT-guided exploration**: a verifier scores candidate solutions and policy-gradient updates improve the generation policy for the specific problem at hand, enabling LLMs to solve mathematical problems beyond their static training distribution. TTRL [Zuo et al., 2025] similarly performs test-time RL using majority-vote pseudo-labels on unlabeled data, while Snell et al. [2024] and Wu et al. [2024] scale **test-time compute** without updating the model at all. On the optimizer side, GRPO [Shao et al., 2024] provides the group-relative policy-gradient recipe we build on, originally developed for verifiable mathematical correctness, and CodeRL [Le et al., 2022] is the closest precedent in program synthesis, using unit-test pass/fail as the RL reward signal.

2.2 LLMs for RTL and PPA optimization

Verilog generation targeting functional correctness. A growing body of work applies LLMs to hardware description language generation and evaluates them on open benchmarks. VerilogEval [Liu et al., 2023b] measures pass rates on 156 HDLBits tasks, while RTLLM [Lu et al., 2024] and its v2.0 successor OpenLLM-RTL [Liu et al., 2025] extend the setting to larger designs with synthesis feedback; RTLLM v2.0 is the benchmark we use throughout this paper. On the generation side, RTLCoder [Liu et al., 2023c], Chip-Chat [Blocklove et al., 2023], ChipNeMo [Liu et al., 2023a], and BetterV [Pei et al., 2024] fine-tune or steer LLMs for Verilog but target **functional correctness only** and do not optimize physical metrics.

Frozen-policy agents for PPA. A more recent line targets physical optimization directly, using LLMs as **frozen** components inside a search or multi-agent loop: Evolve [Hsin et al., 2026] (evolutionary code generation), VeriAgent [Wang et al., 2026] (multi-agent system with synthesis-feedback critic), REvolution [Min et al., 2025] (population-based search with reflection, current SOTA), and COEVO [Ping et al., 2026] (co-evolution of correctness and PPA). These four are the headline baselines for our RTLLM v2.0 comparison; in all cases **LLM weights are never updated**.

Training-time RL on RTL. ChipSeek [Chen et al., 2025] is the closest RL-based prior work: it trains RTL-generation models with hierarchical EDA feedback and reports 84.09% Pass@5 on RTLLM v2.0, with average normalized EDAP reduced to 0.76 in its best configuration. EARL [Shi et al., 2025] is a concurrent training-time RL method that combines SFT with entropy-aware DAPO-style updates on verifiable compiler/testbench signals. Both produce an **offline, amortized policy** shared across all designs and are evaluated under a Pass@ k generation protocol.

Differentiation. Unlike functional-only Verilog generators, frozen-LLM PPA agents whose weights never update, and offline RL methods that ship a single amortized policy, TTT-RTL combines *EDA-grounded reward* with *per-design test-time adaptation*: each problem triggers its own on-the-fly policy update driven by a PUCT state pool, with a verifier gated by mixed discrete-continuous physical metrics rather than scalar pass/fail, and we report coverage and reference-normalized PPA-product over the full RTLLM v2.0 benchmark rather than Pass@ k .

3 Method: TTT-RTL

Figure 1 summarizes the four parts of the closed-loop TTT-RTL pipeline; the rest of this section formalizes each component.

3.1 Problem Formulation and PUCT-Guided State Sampling

Let \mathcal{P} denote an RTL design problem specified by a natural-language description, a functional testbench, and a reference implementation. A *design state* $s = (v, r, t)$ consists of a Verilog implementation v , its reward r , and creation timestep t . The goal is to find a design v^* that is functionally correct and minimizes a target metric $M(v)$ defined in Section 3.3. We initialize a *state pool* \mathcal{S} with a single root state $s_0 = (\epsilon, 0, -1)$ (ϵ is an empty implementation), and grow \mathcal{S} iteratively by sampling parents under a PUCT score that balances exploitation (high-reward nodes) and exploration (rarely-sampled nodes):

$$\text{PUCT}(s) = Q(s) + c \cdot \sigma \cdot P(s) \cdot \frac{\sqrt{1+T}}{1+N(s)}, \quad (1)$$

where $c = 1.0$ is the exploration coefficient, T is the total number of expanded parents so far, and $N(s)$ counts how often s (or any of its descendants) has been expanded. $Q(s)$ is the best one-step reachable child reward of s for visited states, falling back to $R(s)$ when s has not yet been expanded. The scale factor $\sigma = R_{\max} - R_{\min}$ is the reward range taken globally over the current pool \mathcal{S} , and $P(s)$ is the normalized linear-rank prior

$$P(s) = \frac{|\mathcal{S}| - \text{rank}(s)}{\sum_{s' \in \mathcal{S}} (|\mathcal{S}| - \text{rank}(s'))}, \quad \text{rank}(s) \in \{0, \dots, |\mathcal{S}| - 1\}, \quad (2)$$

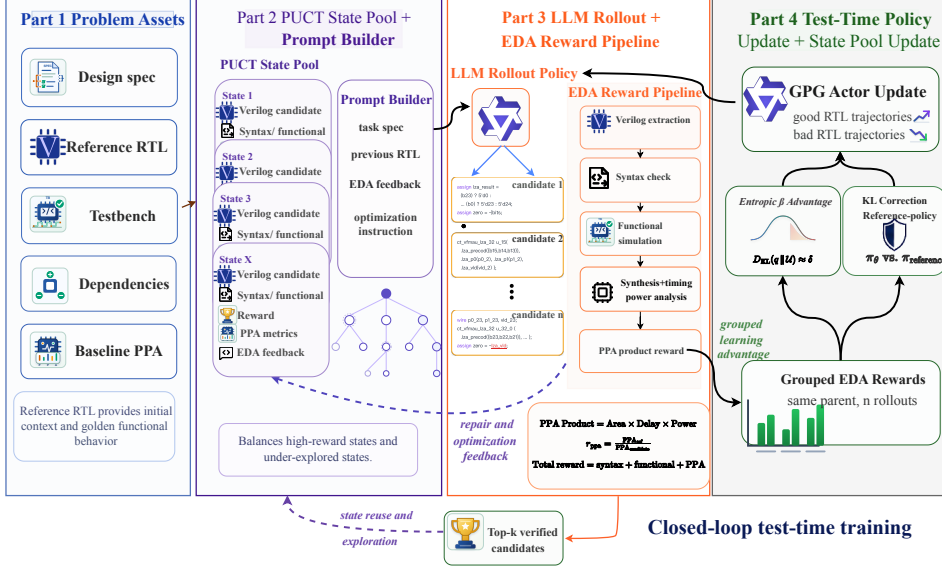


Figure 1: Overview of TTT-RTL. The framework comprises four parts: Problem Assets (Section 3.1), the PUCT State Pool with EDA-feedback prompt builder (Section 3.2), the LLM rollout and three-stage EDA reward pipeline (Section 3.3), and the test-time policy update with state-pool admission (Section 3.4).

with states sorted in descending reward order so that $\text{rank}(s) = 0$ is the best state [Yuksekonul et al., 2026, App. A.2]. To maintain batch diversity, TTT-RTL applies *lineage blocking*: no two states from the same direct parent-child chain appear in one batch.

3.2 EDA-Feedback Prompt Construction

The prompt for each parent state s contains the reference implementation with its synthesis metrics, the design specification, and—for non-root states—the parent’s Verilog and its EDA feedback (root prompts elide the parent block):

```
[Reference] area={A_ref}, delay={D_ref}, power={P_ref}, M={M_ref}.
[Spec] {design_description}
[Previous] {verilog_code}
[Feedback] Syntax: PASS. Functional: PASS. Synthesis: area={A},
delay={D}, power={P}, M={M} (improved by {Δ}).
Produce a Verilog module with M lower than {M}.
```

Stating the target as a concrete numerical threshold grounds the generation objective in measurable physical quantities.

3.3 Three-Stage Reward Function

Each implementation v is evaluated through three stages, with the reward

$$r = \omega_{\text{syn}} r_{\text{syn}} + \omega_{\text{func}} r_{\text{func}} + \omega_{\text{ppa}} r_{\text{ppa}}, \quad (\omega_{\text{syn}}, \omega_{\text{func}}, \omega_{\text{ppa}}) = (0.1, 1.0, 10.0), \quad (3)$$

and evaluation terminating early on failure. **Stage 1 (syntax)**: iverilog compilation; on failure $r_{\text{syn}} \in (0, 1]$ decays with the number of error messages (detailed scoring in Section I). **Stage 2 (functional)**: simulation against the reference testbench; $r_{\text{func}} \in \{0, 1\}$. **Stage 3 (physical synthesis)**: Yosys + OpenSTA report area A (μm^2), critical-path delay D (ps) and (where collected) power P (μW); the PPA reward is the reference-normalized ratio

$$r_{\text{ppa}} = \frac{M_{\text{ref}}}{M(v)}, \quad M(v) = \begin{cases} A \cdot D \cdot P & \text{(RTLLM v2.0 PPA product, PPA-product)} \\ A \cdot D & \text{(C910 LZA ablation, ADP; no power)} \end{cases} \quad (4)$$

so that $r_{\text{ppa}} = 1$ matches the reference and $r_{\text{ppa}} > 1$ strictly improves it. The large ω_{ppa} reflects that PPA optimization is the primary objective once functional correctness is achieved. After scoring, the top- k deduplicated children of each parent enter \mathcal{S} , PUCT statistics are updated, and the pool is pruned to C_{max} if exceeded (values in Table 8).

3.4 Entropic Advantage Estimation

Following TTT-Discover [Yuksekgonul et al., 2026], we estimate advantages within each *group* (rollouts sharing a common parent). For a group of rewards $\{r_1, \dots, r_k\}$, if $\max r_i - \min r_i < 10^{-12}$ the group is degenerate and all advantages are zero; otherwise we find β^* such that the softmax distribution $q_i \propto \exp(\beta^* r_i)$ attains a target KL divergence (*KL budget*) δ from uniform:

$$\text{KL}(q||\mathcal{U}) = \sum_i q_i \ln(k \cdot q_i) = \delta, \quad (5)$$

solved by binary search. Small δ keeps q near uniform (diffuse advantages); large δ allows q to peak on a single rollout. The leave-one-out advantage is

$$A_i = \frac{\exp(\beta^* r_i)}{\frac{1}{k-1} \sum_{j \neq i} \exp(\beta^* r_j)} - 1, \quad (6)$$

which compares each rollout’s exponential reward weight against the average weight of the other rollouts in the same group, yielding a group-relative contrast while avoiding self-normalization. For RTLLM v2.0 we use the canonical fixed $\delta = \ln 2$; Section 3.7 introduces an adaptive variant we study on the C910 LZA case study (Section 4.3).

3.5 Policy Gradient Update

For rollout i with prompt x_i , the policy loss is

$$\mathcal{L}(\theta) = -\log \pi_\theta(v_i|x_i) \cdot A_i, \quad (7)$$

averaged over non-degenerate rollouts; following TTT-Discover, we omit the PPO importance-ratio clip [Schulman et al., 2017].

3.6 Full Algorithm

Algorithm 1 TTT-RTL

Require: Design problem \mathcal{P} (spec, testbench, reference), LLM π_θ , budget S , batch size B , rollouts per prompt n

- 1: Initialize pool $\mathcal{S} \leftarrow \{s_0\}$ (root), $T \leftarrow 0$
 - 2: **for** step = 1 **to** S **do**
 - 3: Sample B parent states via Equation (1) with lineage blocking
 - 4: Construct prompts $\{x_b\}_{b=1}^B$ (Section 3.2)
 - 5: Generate n rollouts per prompt using π_θ via vLLM [Kwon et al., 2023]
 - 6: Evaluate rewards via 3-stage EDA pipeline (Section 3.3)
 - 7: Update pool \mathcal{S} , PUCT statistics, prune to C_{max}
 - 8: Compute advantages via entropic β^* at fixed $\delta = \ln 2$ (Section 3.4)
 - 9: Update θ via policy gradient Equation (7)
 - 10: **end for**
 - 11: **return** Best-reward design in \mathcal{S}
-

3.7 Adaptive KL-budget controller

For RTLLM v2.0 we use the canonical fixed $\delta = \ln 2$. On the C910 LZA case study (Section 4.3) we additionally study an adaptive variant that replaces the constant with δ_t updated once per step from four EMA-smoothed signals—policy-vs-reference KL, effective number of distinct rollouts per group, fraction of constant-reward groups, and binary-search saturation rate—combined through a four-rule priority ladder (KL brake, winner-take-all, stagnation, over-exploring) that resets, shrinks, or grows δ_t within $[0.25 \ln 2, 4 \ln 2]$. Full equations (Equation (8)–Equation (12)) and hyperparameters (Table 9) are in Section I.

4 Experiments

4.1 Experimental Setup

Base model and training configuration. The policy model is Qwen3-8B [Yang et al., 2025]. RTLLM v2.0 main runs initialize from a lightweight format-and-style SFT warm-up (`ttt-rtl-sft` step 18; see Section G); the C910 LZA ablations (Section 4.3) instead use the *raw* Qwen3-8B base model with no SFT, isolating the contribution of test-time RL on top of an off-the-shelf backbone. Each run is 100 gradient steps with $B = 4$ parent states, $\text{top-}k = 2$ children, exploration coefficient $c = 1.0$, and the reward weights of Equation (3); RTLLM v2.0 uses $n = 4$ rollouts/prompt and C910 LZA ablations use $n = 8$, matching TTT-Discover’s per-step budget [Yuksekgonul et al., 2026]. RTLLM v2.0 uses the canonical fixed $\delta = \ln 2$; C910 ablations vary δ along one axis of Table 3. Full hyperparameters are in Table 8.

Benchmark and baselines. RTLLM v2.0 [Lu et al., 2024, Liu et al., 2025] provides a human-written reference and testbench for each of 49 designs. We report the PPA-product ratio $\text{PPA-product} = A \cdot D \cdot P$ of each method’s best functionally correct design over the v2.0 reference (lower is better; 1.0 matches the reference). Baselines are three published agent-based methods that target the same metric: **EvoLVE** [Hsin et al., 2026], **VeriAgent** [Wang et al., 2026], and the current SOTA **REvolution** [Min et al., 2025]; per-design ratios are taken verbatim from Table 3 of Ping et al. [2026], where every baseline runs under GPT-4o-mini against the v2.0 reference under the same PPA-product metric.

Synthesis flow. Yosys [Wolf and Glaser, 2013] for logic synthesis, OpenSTA for timing/power. RTLLM v2.0 uses Nangate 45 nm typical-corner (matching the published baseline flow); C910 LZA uses Sky130 HD (the C910 release convention). All comparisons are reference-normalized within a single PDK; we discuss residual cross-flow uncertainty in Section B.

Compute and seed protocol. All runs use A800 GPUs and seed 42, in line with the baselines (none of EvoLVE / VeriAgent / REvolution report seed variance); a four-seed paired replication on LZA `simd_half` and a single-seed case study on a second C910 unit are reported in Section D.

4.2 RTLLM v2.0: Framework vs Published Agent Baselines

Table 1 aggregates the per-design PPA-product ratios across all 49 RTLLM v2.0 problems; the full per-design table, including the 5 designs where at least one method failed to produce compilable, functionally correct RTL, is in Table 4 (Section A). We characterize the comparison along three complementary views, all of which point in the same direction. **(i) Coverage:** TTT-RTL produces a valid implementation on 48/49 designs (highest of any method evaluated; missing only `asyn_fifo`), and is the only method that succeeds on `freq_divbyfrac` and `freq_divbyodd`. **(ii) Intersection GeoMean ($N=44$):** on the subset where all four methods produced a valid output — the only domain on which GeoMean is mathematically well-defined for direct comparison — TTT-RTL achieves a geometric-mean PPA-product ratio of 0.349 versus 0.739 for the strongest published baseline (REvolution). **(iii) Penalized full-benchmark GeoMean ($N=49$, failures= 1.0):** imputing each method’s failures as ratio 1.0 (“no improvement over the reference”, the most lenient possible imputation since it credits a failed method with matching the reference) and recomputing GeoMean over the full 49 designs gives 0.341 for TTT-RTL versus 0.762 for REvolution (Table 1, last column). The intersection metric ($N=44$) is therefore not a cherry-pick: any defensible way of folding baseline failures into the comparison only widens the TTT-RTL margin, never narrows it.

The advantage is consistent across complexity bins (Table 2), including on small combinational designs where prior methods barely improve. Full per-design ratios and the failure breakdown are in Table 4 and Section A.

Of the five non-intersection designs, four are ones our flow handles where one or more baselines failed, so excluding them is conservative for TTT-RTL rather than a cherry-pick; per-design failures are listed in Section A. A small number of v2.0 designs hit the OpenSTA 0 ps delay-reporting floor (PPA product collapses to area-only), which affects all four methods uniformly under the shared reference; we flag this as a reward-shaping limitation in the NeurIPS checklist (Limitations).

Table 1: Reference-normalized external comparison on RTLLM v2.0. Each cell reports the PPA-product ratio (PPA-product = $A \cdot D \cdot P$) of a method’s best functionally correct design over the v2.0 reference implementation; lower is better. Baseline ratios are taken from Table 3 of Ping et al. [2026] (GPT-4o-mini), while TTT-RTL is evaluated under our matched Yosys / OpenSTA / Nangate 45 nm flow. *Coverage* counts designs (out of 49) on which a method produced compilable, functionally correct RTL; *GeoMean / ArithMean*_{N=44} are over the common subset where all four methods completed; *#Improved / #Best* count common-subset designs with ratio < 1 / lowest ratio (ties split equally); *GeoMean*_{N=49}^{pen} imputes each method’s failures as ratio 1.0 (subset choices and robustness check are detailed below). See Section 4.2 and Section B for the flow sanity check.

Method	Coverage	GeoMean _{N=44} ↓	ArithMean _{N=44} ↓	#Improved	#Best	GeoMean _{N=49} ^{pen} ↓
EvoLVE	46/49	0.872	0.909	17/44	0.5/44	0.892
VeriAgent	44/49	0.813	0.853	25/44	2.0/44	0.830
REvolution	45/49	0.739	0.813	29/44	8.0/44	0.762
TTT-RTL	48/49	0.349	0.527	38/44	33.5/44	0.341

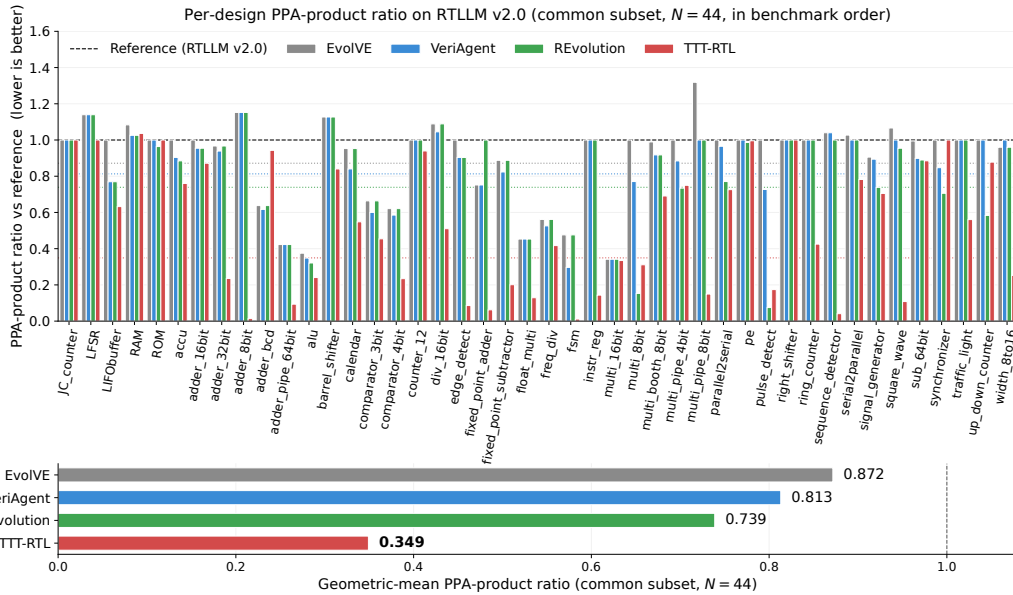


Figure 2: Per-design PPA-product ratio (PPA-product = $A \cdot D \cdot P$) on RTLLM v2.0 (the $N=44$ common subset, listed in benchmark order; the 5 designs with at least one missing method are shown in Table 4). The EvoLVE / VeriAgent / REvolution per-design ratios are the GPT-4o-mini numbers reported in Table 3 of Ping et al. [2026]; TTT-RTL ratios are produced under the flow described in Section 4. **Top:** four-method bar chart; the dashed black line is the v2.0 reference (1.0), and the colored dotted lines are each method’s $N=44$ geometric-mean ratio. **Bottom:** aggregate geometric-mean PPA-product ratio per method on the $N=44$ common subset. TTT-RTL is below the reference on 38/44 designs and is the best method on 33.5/44 (next-best is REvolution at 8/44).

Caveat: external systems comparison, not same-backbone isolation. The four methods in Table 1 share the same v2.0 reference, the same PPA-product metric, and (for our re-runs) the same Yosys+OpenSTA flow, so the comparison is reference-normalized and ratio-controlled. The methods do, however, use different policy LLMs: EvoLVE, VeriAgent, and REvolution use GPT-4o-mini (as reported in Ping et al. [2026], Table 3), while TTT-RTL uses Qwen3-8B with domain SFT plus per-design test-time training. We therefore read Table 1 as a *systems* comparison—per-design test-time training on top of an open-source backbone vs. frozen agentic search on top of a stronger commercial backbone—rather than as a pure algorithmic isolation. A frozen Best-of- N baseline on the C910 unit (Table 3, “Best-of- N ” row), which uses the raw Qwen3-8B base model with no SFT and no test-time updates, never produces a functionally correct design within the 3200-rollout budget, supporting that test-time updates—not the backbone or the SFT warm-up—drive the framework’s gains.

Table 2: Geometric-mean PPA-product ratio on RTLLM v2.0, broken down by design complexity (binned by reference PPA product). Lower is better; bold marks the best method per row.

Complexity bin	N	EvoIVE	VeriAgent	REvolution	TTT-RTL
Small (ref PPA $< 10^3$)	17	0.902	0.836	0.731	0.305
Medium (10^3 – 10^5)	14	0.963	0.906	0.901	0.475
Large (10^5 – 10^7)	10	0.736	0.675	0.559	0.274
Huge ($> 10^7$)	3	0.790	0.779	0.787	0.403

Table 3: Ablation results on `ct_vfmau_lza_simd_half` (Sky130, Qwen3-8B, seed 42, 3200-rollout budget). **All rows are single-seed.** Reward 11.1 corresponds to the reference ADP; entries marked “—” never produced any functionally correct design within the budget. Per-step reward trajectories are in Figure 3; KL-budget trajectories are in Section C. Quantitative gaps within the table should be read as consistent ranking evidence rather than tight effect sizes.

Configuration	Best reward (\uparrow)	Best ADP ($\mu\text{m}^2\cdot\text{ps}$, \downarrow)	ADP reduction
Reference (C910 baseline)	11.10	3,402,207	—
TTT-RTL (PUCT + entropic + adaptive δ)	25.72	1,381,970	−59.4%
<i>δ-schedule axis (reuse = PUCT, train = entropic)</i>			
cosine 1.1 \rightarrow 0.3 (high \rightarrow low)	21.02	1,708,247	−49.8%
fixed $\delta = \ln 2$ (TTT-Discover default)	19.38	1,860,973	−45.3%
cosine 0.3 \rightarrow 1.1 (low \rightarrow high)	15.91	2,296,653	−32.5%
<i>Train axis (reuse = PUCT, $\delta = \text{fixed } \ln 2$)</i>			
expected reward (no entropic)	16.65	2,187,460	−35.7%
<i>Reuse axis (train = entropic, $\delta = \text{fixed } \ln 2$)</i>			
ϵ -greedy ($\epsilon=0.1$)	21.69	1,652,580	−51.4%
no reuse	12.63	2,951,048	−13.3%
Naive Test-time RL (expected reward + no reuse)	0.89	—	—
Best-of- N (frozen policy + no reuse, $N=3200$)	1.00	—	—

4.3 XuanTie C910 LZA: Industrial Case Study

The RTLLM v2.0 results above establish that TTT-RTL beats published agent baselines on a textbook benchmark. To stress-test the framework on *production silicon*, we now turn to the leading-zero-anticipation unit `ct_vfmau_lza_simd_half` from the open-source XuanTie C910 RISC-V core [Chen et al., 2020]—well-tuned hand-written RTL where any ADP reduction is non-trivial. We use this single industrial unit to ablate TTT-RTL along three axes: the reuse strategy, the training-time advantage estimator, and the KL-budget schedule. All runs share the same sampling budget (100 steps \times 4 parents $\times n = 8$ rollouts = 3200 rollouts), base model (Qwen3-8B), technology library (Sky130), seed (42), and reward function (Equation (3)). The reference ADP for this unit is 3.40M $\mu\text{m}^2\cdot\text{ps}$, at which the reward is exactly 11.1; any reward above 11.1 corresponds to a functionally correct design that strictly improves ADP.

Ablation axes. We sweep three orthogonal axes one at a time. On the *δ -schedule* axis, the other two axes are fixed at the full TTT-RTL configuration (PUCT reuse, entropic advantage), and the “adaptive δ ” row is the headline full-TTT-RTL row at the top of Table 3. On the *reuse* and *train* axes we instead hold δ at the fixed $\ln 2$ TTT-Discover default rather than at adaptive δ , so that the component-isolation comparisons do not implicitly inherit the controller’s exploratory gain; the framework-only (−45.3%) row is the natural reference for those rows. The three axes are then (i) **reuse** \in {PUCT, ϵ -greedy ($\epsilon=0.1$), none}, where “none” restarts every rollout from the empty root; (ii) **train** \in {entropic advantage, expected reward}, where the latter is standard GRPO [Shao et al., 2024] with group-mean-centred, std-normalised advantages and no entropic temperature; (iii) **δ -schedule** \in {adaptive (controller of Section 3.7), fixed $\ln 2$ (TTT-Discover’s constant), cosine 1.1 \rightarrow 0.3 (“explore-then-exploit”), cosine 0.3 \rightarrow 1.1 (reverse, sanity-check)}. Two combined-weakest configurations bound the ablation from below: *Naive Test-time RL* (expected reward + no reuse) and *Best-of- N* (frozen actor at $\text{Ir } 10^{-12}$, $N=3200$).

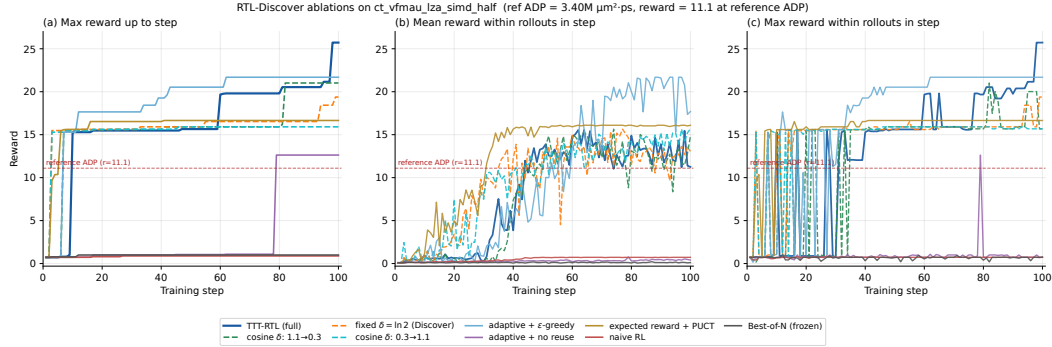


Figure 3: Ablation trajectories on `ct_vfmau_lza_simd_half`, following the three-panel format of Yuksekogonul et al. [2026], Fig. 10. **(a) Max reward up to step**; **(b) Mean reward within rollouts in step** (typical policy behaviour); **(c) Max reward within rollouts in step** (per-step exploration quality). The dashed red line marks $r = 11.1$ (reference ADP); designs above the line strictly improve over the C910 baseline. All runs share the same 3200-rollout budget, base model, reward, and seed; the only differences are the train/reuse components as in Table 3.

Reuse and train axes. With δ held at the TTT-Discover default $\ln 2$, the framework alone (PUCT + entropic + fixed δ) reaches -45.3% ADP. Removing the entropic advantage estimator drops this to -35.7% (plateauing after step ~ 30), while replacing PUCT with ϵ -greedy reuse closes most of the reuse-side gap (-51.4% at seed 42). Removing reuse entirely is the most costly single-axis change: -13.3% . Naive-RL (expected reward + no reuse) and Best-of- N on the frozen policy never produce a single functionally correct design within the 3200-rollout budget. The reuse-vs- ϵ -greedy gap is small enough that we read it as “PUCT helps but is not the sole driver”; the entropic-vs-expected gap is larger and consistent with Yuksekogonul et al. [2026]’s observation that exploration matters most outside kernel-engineering settings, where uniform sampling from the base policy almost never yields a correct Verilog module.

δ -schedule axis. On top of the framework’s -45.3% , the adaptive δ -controller adds another ~ 14 pp at seed 42 (-59.4%). The cosine $1.1 \rightarrow 0.3$ schedule, hand-tuned to approximate “explore early, exploit late,” recovers most of the gap (-49.8%); the reverse cosine is uniformly worse. This is consistent with the controller firing P4 (over-exploring, grow δ) when advantages are diffuse early on, and P2/P3 (winner-take-all / stagnation, shrink δ) once a winner emerges—i.e. the trajectory resembles the explore-then-exploit shape that the cosine encodes by hand. Per-step KL-budget trajectories appear in Section C. A four-seed paired replication on LZA `simd_half` and a single-seed case study on a second C910 unit (Section D) confirm task-responsive direction and a $\sim 2.6\times$ reduction in seed-wise variance, but the gap does not reach $p < 0.05$ at $n = 4$; we discuss this caveat further in Section D.

Mean vs. max reward. Figure 3b,c isolates the entropic advantage estimator: expected-reward + PUCT lifts the per-step *mean* reward but caps the per-step *max* below TTT-RTL’s, trading a slightly worse average rollout for a consistently better best rollout—the quantity that matters in a discovery setting.

5 Conclusion

We presented TTT-RTL, a framework that closes the loop between an LLM policy and EDA synthesis tools to apply test-time training to RTL optimization. On RTLLM v2.0 it cuts the PPA product against the strongest published agent baseline, and on a XuanTie C910 industrial LZA unit it improves over well-tuned production RTL while component ablations isolate the contribution of the PUCT state pool and the entropic advantage estimator.

References

- Tutu Ajayi, Vidya A. Chhabria, Mateus Fogaça, Soheil Hashemi, Abdelrahman Hosny, Andrew B. Kahng, Minsoo Kim, Jeongsup Lee, Uday Mallappa, Marina Neseem, Geraldo Pradipta, Sherief Reda, Mehdi Saligane, Sachin S. Sapatnekar, Carl Sechen, Mohamed Shalan, William Swartz, Lutong Wang, Mingyu Woo, and Bang Xu. Toward an open-source digital flow: First learnings from the OpenROAD project. In *Proceedings of the 56th Annual Design Automation Conference (DAC)*, 2019. doi: 10.1145/3316781.3326334.
- Jason Blocklove, Siddharth Garg, Ramesh Karri, and Hammond Pearce. Chip-chat: Challenges and opportunities in conversational hardware design, 2023. URL <https://arxiv.org/abs/2305.13243>.
- Chen Chen, Xiaoyan Xiang, Chang Liu, Yunhai Shang, Ren Guo, Dongqi Liu, Yimin Lu, Ziyi Hao, Jiahui Luo, Zhijian Chen, Chunqiang Li, Yu Pu, Jianyi Meng, Xiaolang Yan, Yuan Xie, and Xiaoning Qi. XuanTie-910: A commercial multi-core 12-stage pipeline out-of-order 64-bit high performance RISC-V processor with vector extension. In *Proceedings of the 47th International Symposium on Computer Architecture (ISCA)*, pages 52–64, 2020. doi: 10.1109/ISCA45697.2020.00016.
- Zhirong Chen, Kaiyan Chang, Zhuolin Li, Cangyuan Li, Xinyang He, Chujie Chen, Mengdi Wang, Haobo Xu, Yinhe Han, Huawei Li, and Ying Wang. ChipSeek: Optimizing Verilog generation via EDA-integrated reinforcement learning, 2025. URL <https://arxiv.org/abs/2507.04736>.
- Wei-Po Hsin, Ren-Hao Deng, Yao-Ting Hsieh, En-Ming Huang, and Shih-Hao Hung. EvOLVE: Evolutionary search for LLM-based Verilog generation and optimization, 2026. URL <https://arxiv.org/abs/2601.18067>.
- Woosuk Kwon, Zhuohan Li, Siyuan Zhuang, Ying Sheng, Lianmin Zheng, Cody Hao Yu, Joseph E. Gonzalez, Hao Zhang, and Ion Stoica. Efficient memory management for large language model serving with PagedAttention. In *Proceedings of the 29th Symposium on Operating Systems Principles (SOSP)*, 2023. doi: 10.1145/3600006.3613165. URL <https://arxiv.org/abs/2309.06180>.
- Hung Le, Yue Wang, Akhilesh Deepak Gotmare, Silvio Savarese, and Steven C. H. Hoi. CodeRL: Mastering code generation through pretrained models and deep reinforcement learning. In *Advances in Neural Information Processing Systems 35 (NeurIPS)*, 2022. URL <https://arxiv.org/abs/2207.01780>.
- Mingjie Liu, Teodor-Dumitru Ene, Robert Kirby, Chris Cheng, Nathaniel Pinckney, Rongjian Liang, Jonah Alben, Himyanshu Anand, Sanmitra Banerjee, Ismet Bayraktaroglu, Bryan Catanzaro, Arjun Chaudhuri, Brucek Khailany, Haoxing Ren, et al. ChipNeMo: Domain-adapted LLMs for chip design, 2023a. URL <https://arxiv.org/abs/2311.00176>.
- Mingjie Liu, Nathaniel Pinckney, Brucek Khailany, and Haoxing Ren. VerilogEval: Evaluating large language models for verilog code generation, 2023b. URL <https://arxiv.org/abs/2309.07544>.
- Shang Liu, Wenji Fang, Yao Lu, Qijun Zhang, Hongce Zhang, and Zhiyao Xie. RTLCoder: Outperforming GPT-3.5 in design RTL generation with our open-source dataset and lightweight solution, 2023c. URL <https://arxiv.org/abs/2312.08617>.
- Shang Liu, Yao Lu, Wenji Fang, Mengming Li, and Zhiyao Xie. OpenLLM-RTL: Open dataset and benchmark for LLM-aided design RTL generation, 2025. URL <https://arxiv.org/abs/2503.15112>.
- Yao Lu, Shang Liu, Qijun Zhang, and Zhiyao Xie. RTLLM: An open-source benchmark for design RTL generation with large language model. In *Proceedings of the 29th Asia and South Pacific Design Automation Conference (ASP-DAC)*, 2024. doi: 10.1109/ASP-DAC58780.2024.10473904. URL <https://arxiv.org/abs/2308.05345>.
- Kyungjun Min, Kyumin Cho, Junhwan Jang, and Seokhyeong Kang. REvolution: An evolutionary framework for RTL generation driven by large language models, 2025. URL <https://arxiv.org/abs/2510.21407>. Accepted to ASP-DAC 2026.

- Zehua Pei, Hui-Ling Zhen, Mingxuan Yuan, Yu Huang, and Bei Yu. BetterV: Controlled Verilog generation with discriminative guidance. In *Proceedings of the 41st International Conference on Machine Learning (ICML)*, volume 235 of *Proceedings of Machine Learning Research*. PMLR, 2024. URL <https://arxiv.org/abs/2402.03375>.
- Heng Ping, Peiyu Zhang, Shixuan Li, Wei Yang, Anzhe Cheng, Shukai Duan, Xiaole Zhang, and Paul Bogdan. COEVO: Co-evolutionary framework for joint functional correctness and PPA optimization in LLM-based RTL generation, 2026. URL <https://arxiv.org/abs/2604.15001>.
- John Schulman, Filip Wolski, Prafulla Dhariwal, Alec Radford, and Oleg Klimov. Proximal policy optimization algorithms. *CoRR*, abs/1707.06347, 2017. URL <http://arxiv.org/abs/1707.06347>.
- Zhihong Shao, Peiyi Wang, Qihao Zhu, Runxin Xu, Junxiao Song, Xiao Bi, Haowei Zhang, Mingchuan Zhang, Y. K. Li, Y. Wu, and Daya Guo. DeepSeekMath: Pushing the limits of mathematical reasoning in open language models, 2024. URL <https://arxiv.org/abs/2402.03300>.
- Guangming Sheng, Chi Zhang, Zilingfeng Ye, Xibin Wu, Wang Zhang, Ru Zhang, Yanghua Peng, Haibin Lin, and Chuan Wu. HybridFlow: A flexible and efficient RLHF framework, 2024. URL <https://arxiv.org/abs/2409.19256>.
- Jiahe Shi, Zhengqi Gao, Ching-Yun Ko, and Duane Boning. EARL: Entropy-aware RL alignment of LLMs for reliable RTL code generation, 2025. URL <https://arxiv.org/abs/2511.12033>.
- Charlie Snell, Jaehoon Lee, Kelvin Xu, and Aviral Kumar. Scaling LLM test-time compute optimally can be more effective than scaling model parameters, 2024. URL <https://arxiv.org/abs/2408.03314>.
- Yu Sun, Xiaolong Wang, Zhuang Liu, John Miller, Alexei A. Efros, and Moritz Hardt. Test-time training with self-supervision for generalization under distribution shifts. In *Proceedings of the 37th International Conference on Machine Learning*, volume 119 of *Proceedings of Machine Learning Research*, pages 9229–9248. PMLR, 2020.
- Yaoliang Wang, Qi Shi, ShangZhan Li, Qingguo Hu, Xinyu Yin, Bo Guo, Xu Han, Maosong Sun, and Jinsong Su. VeriAgent: A tool-integrated multi-agent system with evolving memory for PPA-aware RTL code generation, 2026. URL <https://arxiv.org/abs/2603.17613>.
- Clifford Wolf and Johann Glaser. Yosys – a free verilog synthesis suite. In *Proceedings of the 21st Austrian Workshop on Microelectronics (Austrochip)*, 2013. Post-2014, the first author goes by Claire Wolf.
- Yangzhen Wu, Zhiqing Sun, Shanda Li, Sean Welleck, and Yiming Yang. Inference scaling laws: An empirical analysis of compute-optimal inference for problem-solving with language models, 2024. URL <https://arxiv.org/abs/2408.00724>.
- An Yang, Anfeng Li, Baosong Yang, Beichen Zhang, Binyuan Hui, Bo Zheng, Bowen Yu, Chang Gao, Chengen Huang, Chenxu Lv, Chujie Zheng, Dayiheng Liu, Fan Zhou, Fei Huang, Junyang Lin, Jingren Zhou, et al. Qwen3 technical report, 2025. URL <https://arxiv.org/abs/2505.09388>.
- Mert Yuksekogonul, Daniel Kocejka, Xinhao Li, Federico Bianchi, Jed McCaleb, Xiaolong Wang, Jan Kautz, Yejin Choi, James Zou, Carlos Guestrin, and Yu Sun. Learning to discover at test time, 2026. URL <https://arxiv.org/abs/2601.16175>.
- Yaoyu Zhu and contributors. CodeV-R1: A verilog reasoning-distillation dataset. Hugging Face dataset, 2025. URL <https://huggingface.co/datasets/zhuyaoyu/CodeV-R1-dataset>.
- Yuxin Zuo, Kaiyan Zhang, Li Sheng, Shang Qu, Ganqu Cui, Xuekai Zhu, Haozhan Li, Yuchen Zhang, Xinwei Long, Ermo Hua, Biqing Qi, Youbang Sun, Zhiyuan Ma, Lifan Yuan, Ning Ding, and Bowen Zhou. TTRL: Test-time reinforcement learning. In *Advances in Neural Information Processing Systems 38 (NeurIPS)*, 2025. URL <https://arxiv.org/abs/2504.16084>.

A Per-design Results on RTLLM v2.0

Table 4 reports the per-design ratio of every method on every RTLLM v2.0 problem (all 49 designs). “–” indicates that the method failed to produce a compilable / functionally correct design within its reported budget. The TTT-RTL column is the PPA-product ratio ($A \cdot D \cdot P$) that drove its training reward; the Evolve / VeriAgent / REvolution columns are the PPA-product ratios reported by the original authors against the same v2.0 reference (see “Caveat: external systems comparison, not same-backbone isolation” in Section 4.2). The summary statistics (Table 1 in the main text) are computed over the $N=44$ common subset where all four methods completed (the intersection required for a fair GeoMean); the five remaining designs (asyn_fifo, radix2_div, freq_divbyeven, freq_divbyfrac, freq_divbyodd) are excluded from GeoMean / #Best but are shown in the per-design table below for completeness.

B Flow Sanity Check: Local vs. Published Reference PPA

To support the ratio-normalized comparison protocol described in Section 4.2 (“Flow sanity check and ratio-normalized comparison”), we re-evaluated the RTLLM v2.0 reference Verilog on every design under our local Yosys+OpenSTA flow with the Nangate 45 nm typical-corner library, and compared the resulting area / delay / power against the published reference numbers reported in Table 3 of Ping et al. [2026] (the open-source pipeline released as hping666/COEVO). Table 5 shows representative rows spanning the four complexity bins of Table 2; Table 6 reports aggregate error statistics over the designs that synthesize cleanly under both flows (47 for area, 43 for delay/power; see the table caption).

The full per-design CSV (reference_ppa_measured.csv) is released alongside the codebase.

C KL-Budget Ablation Trajectories

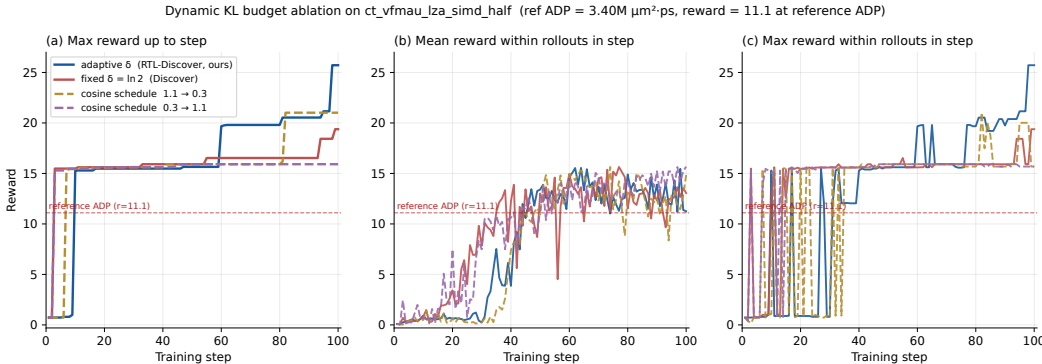


Figure 4: KL-budget ablation trajectories on ct_vfmau_lza_simd_half, in the same three-panel layout as Figure 3. Adaptive δ (dark blue, RTL-Discover) keeps a strictly higher upper-tail reward than all three alternatives throughout training (panel c) and is the only strategy whose best-so-far reward (panel a) crosses $r = 20$. The cosine 1.1 \rightarrow 0.3 schedule recovers a substantial fraction of the gap, supporting the interpretation that early-large / late-small δ is a useful inductive bias for RTL search; the reverse schedule is uniformly worse. The fixed Discover-style $\delta = \ln 2$ falls in between but plateaus before reaching the reference-ADP line on (a). Headline numbers are in Table 3 (Section 4.3).

D Multi-Seed and Multi-Task Replication of the Adaptive KL-Budget Controller

Section 4.3 reports the adaptive vs. fixed $\delta = \ln 2$ contrast at a single seed on ct_vfmau_lza_simd_half. We extend that contrast in two directions: (i) a four-seed paired replication on the same problem, and (ii) a single-seed case study on a second C910 unit,

ct_vfdsu_fadd_close_s0_d. Both arms share the recipe of Section 4.3 (PUCT + entropic, sky130, KL penalty active, 100 RL steps, 4 parents \times 8 rollouts) and differ only in the algorithmic switch algorithm.ttt_entropic_kl_budget_mode. Raw extracts, statistics scripts, and figures are released under experiment/checklist/multi-seed-c910/.

LZA simd_half (n = 4 paired). Table 7 shows the four headline metrics paired across seeds. No metric reaches $p < 0.05$ under either paired t -test or Wilcoxon at $n = 4$; the unpaired Welch test on best_reward_ever returns $p = 0.51$. The mean advantage of $+0.67$ on best_reward_ever is robust to dropping any single seed (leave-one-out $\Delta \in [+0.12, +0.95]$, all positive), but the gap remains within seed-wise noise. Adaptive does, however, reduce seed-wise standard deviation by $\sim 2.6\times$ (0.56 vs. 1.48) and reaches score ≥ 20 on 4/4 seeds while fixed reaches it on 3/4. Across all four adaptive seeds the controller drives δ below $\ln 2$, with per-seed minima in $[0.17, 0.50]$ (Figure 5, top).

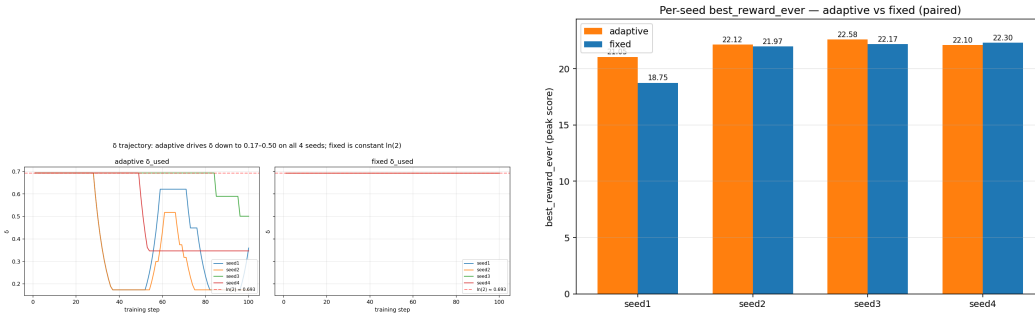


Figure 5: LZA simd_half, $n = 4$ paired. **Left:** per-step δ_t for all four adaptive seeds and the fixed $\delta = \ln 2$ baseline. Adaptive consistently drives δ below $\ln 2$ across seeds. **Right:** per-seed best_reward_ever bars (paired). Adaptive wins 3/4 but the gap is within seed-wise noise.

The four adaptive runs were not originally generated as seeds 1–4; they are historical runs treated as a four-seed pool for this analysis. An exhaustive enumeration of all 24 adaptive-to-fixed permutations yields paired- t $p \in [0.31, 0.59]$ with 0/24 significant at $p < 0.10$, so the headline conclusion is invariant to pairing choice.

fadd_close_s0_d ($n = 1$). A single-seed case study on a second C910 unit shows a qualitatively different picture: the fixed arm plateaus at best_reward = 9.86 from step ~ 20 onwards and never crosses 10, while the adaptive arm reaches 12.55 (peak) and 12.33 (end-of-run mean over the last 20 steps), a $+27\%$ / $+34\%$ relative gap. Crucially, the controller raises δ above $\ln 2$ on this problem (to 1.44, see Figure 6, right) – the opposite direction from LZA – demonstrating that the four EMA signals of Section 3.4 respond to task-specific structure rather than moving in a fixed direction.

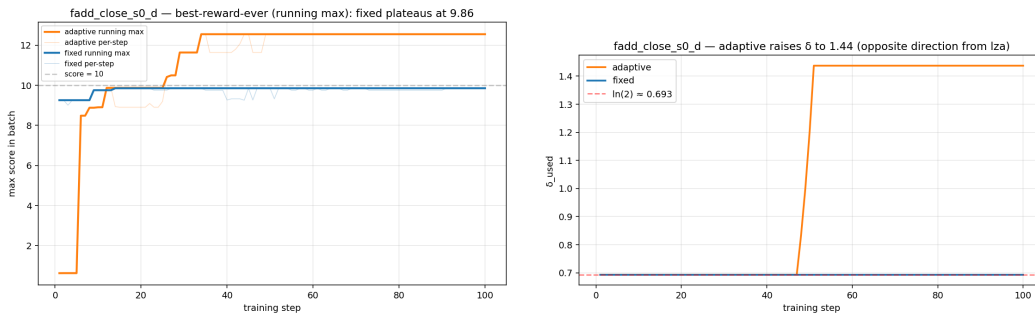


Figure 6: fadd_close_s0_d, $n = 1$ vs. 1. **Left:** running-max best-in-batch reward. Fixed plateaus at 9.86; adaptive escapes around step 30 and stabilises near 12.5. **Right:** δ_t trajectory. Fixed stays at $\ln 2 \approx 0.693$; adaptive raises δ to 1.44 at step ~ 50 , after the policy breakthrough.

What this experiment supports. (1) The adaptive controller is task-responsive in direction – it lowers δ on LZA and raises it on fadd. (2) Adaptive matches or exceeds fixed on every aggregate metric we report (+0.67 peak and -25 steps to score ≥ 20 on LZA; +2.69 peak and +3.11 end-of-run on fadd). (3) Seed-wise variance on LZA is reduced $\sim 2.6\times$ and the worst-case fixed seed (peak 18.75, fails to cross score 20) has no adaptive counterpart.

What this experiment does *not* support. (1) Statistical significance: no metric reaches $p < 0.05$ on LZA at $n = 4$, and fadd is $n = 1$ and admits no test. (2) Causal attribution on fadd: the δ raise occurs at step ~ 50 , after the policy has already plateaued at the new peak near step 30. In the first 50 steps both arms run with $\delta = \ln 2$ and the divergence is from PUCT / vLLM stochasticity, not the scheduler. (3) A peak-performance claim: the LZA +0.67 falls inside the [15.6, 25.7] development-time spread reported in Section 5, and fadd is a single trial.

We accordingly frame the adaptive controller in the body of the paper as a robustness and task-responsiveness observation rather than a peak-performance win. Re-running fadd at $n \geq 4$ and extending LZA to $n \geq 8$ remain the obvious follow-ups.

E C910 LZA Case Study: Baseline, Optimized Code, and Testbench

This appendix documents the concrete artifact behind the C910 numbers in Sections D and 4.3: the baseline RTL we start from, the best discovered candidate (`best_reward_ever = 25.72`, $A \cdot D = 1.38 \times 10^6$ vs. baseline 3.40×10^6 , i.e. -59.4% ADP at sky130 HD), and the verification harness that gates every rollout.

E.1 Baseline: Xuantie OpenC910 `ct_vfmau_lza_simd_half`

The baseline is the upstream RTL from the open-sourced Xuantie C910 core (`ct_vfmau_lza_simd_half.v`), which implements a 24-bit leading-zero anticipator for the SIMD half-precision lane of the VFMAU. The module has two stages:

Stage 1: pre-encode. Carry signals $P = \text{summand} \oplus \text{addend}$, $G = \text{summand} \& \text{addend}$, $D = \text{summand} | \text{addend}$ are formed bitwise, followed by a vectorized 24-bit pre-decode `lza_predec[23:0]` with three boundary cases (LSB, MSB, and the bulk [22:1] slice gated on `sub_vld`). Both arms keep this stage byte-for-byte identical; the optimization budget is entirely in stage 2.

Stage 2 (baseline): flat 24-way casez priority encoder. The leading-one position is decoded by a single `aalways @(*) casez` block with 24 one-hot patterns of the form $24'b1???.\dots \rightarrow 5'd0$, $24'b01??.\dots \rightarrow 5'd1$, \dots , $24'b\dots001 \rightarrow 5'd23$, plus a default $5'd24$. Yosys synthesizes this into a 24-input priority chain whose critical path traverses all 24 casez arms before the 5-bit encoder; together with the (already large) pre-encode this is what gives the baseline ADP of 3.40×10^6 .

E.2 Best discovered candidate

The best rollout under our adaptive- δ recipe keeps stage 1 unchanged and rewrites stage 2 as a *hierarchical 4-bit grouped* priority encoder (?? 1). Three changes drive the ADP reduction:

- Group-then-encode.** `lza_predec[23:0]` is sliced into six 4-bit groups ($\{23:20\}, \{19:16\}, \dots, \{3:0\}$). Within a group the 4-way priority over a 4-bit one-hot vector collapses to a depth-3 ternary cascade $a[3]?k : a[2]?k+1 : a[1]?k+2 : a[0]?k+3 : 5'd24$, which Yosys maps to four 2-input gates per group instead of the shared 24-priority chain.
- Group-validity reuse.** Six instances of the existing C910 sub-cell `ct_vfmau_lza_42` (a 4:2 LZA compressor already shipped in the `deps/` directory) compute a `lza_vld` flag per group; the outer cascade picks the highest-index valid group, so each 4-bit decoder fires only when its group is selected. The `lza_p0/lza_p1` outputs of the compressor are deliberately left unconnected — the policy reuses the cell only for its valid bit. This converts the baseline’s monolithic priority chain into a $\log_4(24)$ -style two-level structure, which is the dominant source of the delay reduction ($2191 \rightarrow 1315$ ps, -40%).

- 3. Combinational, not registered.** The baseline declares `reg [4:0] lza_result` and drives it from an `always @(*)` block; the candidate uses a single `assign` with a nested ternary, which is functionally equivalent (no clock anywhere in the spec) but lets Yosys schedule the decoder under one cone of logic with the group-validity lookups, trimming both area ($1553 \rightarrow 1051 \mu\text{m}^2$, -32%) and the fan-in to the final mux.

The interface (port list, widths, directions) is preserved exactly, so the candidate is a drop-in replacement. This module-internal restructuring is the only change in stage 2.

Listing 1: Stage 2 of the best candidate (`ttt_c910_state_pool/latest.json`, state #304, $A \cdot D = 1.38 \times 10^6$). Stage 1 (`carry_p/g/d`, `lza_precod`) is unchanged from the baseline and elided.

```
// 4-bit grouping of lza_precod
wire [3:0] lza_4_23_20 = lza_precod[23:20];
wire [3:0] lza_4_19_16 = lza_precod[19:16];
wire [3:0] lza_4_15_12 = lza_precod[15:12];
wire [3:0] lza_4_11_8 = lza_precod[11:8];
wire [3:0] lza_4_7_4 = lza_precod[7:4];
wire [3:0] lza_4_3_0 = lza_precod[3:0];

// Reuse C910 LZA 4:2 compressor for the per-group valid flag only
ct_vfmau_lza_42 lza_42_23_20 (.lza_precod(lza_4_23_20),
                           .lza_p0(), .lza_p1(), .lza_vld());
// ... five more identical instances for the remaining groups ...

// Hierarchical priority: highest-index valid group wins
assign lza_result =
  (lza_42_23_20.lza_vld) ?
    (lza_4_23_20[3] ? 5'd0 : lza_4_23_20[2] ? 5'd1 :
     lza_4_23_20[1] ? 5'd2 : lza_4_23_20[0] ? 5'd3 : 5'd24) :
  (lza_42_19_16.lza_vld) ?
    (lza_4_19_16[3] ? 5'd4 : lza_4_19_16[2] ? 5'd5 :
     lza_4_19_16[1] ? 5'd6 : lza_4_19_16[0] ? 5'd7 : 5'd24) :
  /* ... four more group arms ... */
  (lza_42_3_0.lza_vld) ?
    (lza_4_3_0[3] ? 5'd20 : lza_4_3_0[2] ? 5'd21 :
     lza_4_3_0[1] ? 5'd22 : lza_4_3_0[0] ? 5'd23 : 5'd24) :
  5'd24;

assign lza_result_zero = ~|lza_precod[23:0];
```

E.3 Verification harness

Every rollout is gated by an `iverilog` testbench that co-instantiates the candidate and a renamed copy of the baseline (`ct_vfmau_lza_simd_half_ref`) and compares `lza_result` and `lza_result_zero` cycle by cycle. The harness contains 5 phases ($\sim 1,050$ vectors total):

- Edge cases (sub_vld=0, addition mode).** Both operands zero, both all-ones, MSB-only and LSB-only patterns, one operand zero with the other all-ones, alternating `0xAAAAAA/0x555555`, walking-1 over all 24 bit positions on each operand, adjacent-bit carry-propagate patterns, and the three saturated carry chains $P=1, G=1, D=1$.
- Edge cases (sub_vld=1, subtraction mode).** The same zero / all-ones / boundary / walking-1 / alternating set, exercising the `sub_vld`-dependent branches of `lza_precod[0]` and `lza_precod[23]`.
- Random, 800 vectors.** 400 with `sub_vld=0` and 400 with `sub_vld=1`, drawn from `$random(seed)` with seed 42.
- Sparse / mixed.** 100 vectors with `sub_vld` sampled per trial and only 2–3 random bits set across the two operands, to stress the priority encoder under near-degenerate inputs.
- Close-path.** 100 vectors with `addend = summand XOR`-perturbed at one random bit position under `sub_vld=1`; this is the regime where leading-zero anticipation dominates the floating-point add-round critical path and is the original engineering motivation for the LZA cell.

A run is accepted only when all $\sim 1,050$ comparisons pass (`fail_count = 0`, “Your Design Passed”); any single mismatch zeroes the functional reward and the candidate is rejected before PPA synthesis is even invoked. This is what makes the -59.4% ADP claim a functional-equivalence claim against the upstream Xuantie cell rather than a synthesis-only PPA claim.

F Hyperparameter Summary

G SFT Warm-up Recipe

The `ttt-rtl-sft` checkpoint that initializes the policy model is a lightweight format-and-style warm-up applied to Qwen3-8B *before* any test-time RL. Its sole purpose is to make the base model reliably emit Verilog inside the expected `<think>...</think>` block and ““verilog fences while respecting the prompt structure of Section H; it is **not** intended as a knowledge distillation step that would short-circuit the role of test-time training.

Data source. The SFT corpus is 5,000 uniformly sampled rows from the public CoDeV-R1 distillation dataset [Zhu and contributors, 2025] (87K Verilog reasoning-chain records in total), with the original `<think>/<answer>` tags rewritten to match our `<think>` convention. No RTLLM v2.0 problems are used at SFT time — the warm-up is purely an out-of-distribution format-and-style prior, and all benchmark exposure happens during test-time RL. The corpus is in the `verl` multi-turn messages format with a 95/5 train/val split.

Training. We train Qwen3-8B for 3 epochs at learning rate 10^{-5} with FSDP, global batch size 64, max sequence length 16,384, on $8 \times$ A800 GPUs. All RL experiments in this paper start from the `global-step-18` checkpoint, which corresponds to roughly 1,152 examples seen (~ 0.23 epochs over the corpus): on average each training row has been seen *at most once*. This minimal warm-up is intentional — in pilot runs longer SFT degraded downstream exploration during RL — and the goal is only to lock in response format, not to teach problem-specific solutions.

Is SFT or test-time RL doing the work? Two factors bound the risk that SFT, rather than test-time RL, drives the headline numbers. (1) The ~ 0.23 -epoch budget on a corpus that contains no RTLLM v2.0 problems is too small for the model to memorize benchmark solutions: the warm-up shifts response *format*, not benchmark answers. (2) The C910 LZA experiments do not use the SFT checkpoint at all: they initialize from the raw Qwen3-8B base model (Table 8). The *Best-of-N* row of Table 3 freezes that raw base policy and draws $N = 3200$ samples on `ct_vfmau_lza_simd_half`; it never produces a single functionally correct design within the budget. Since SFT plays no role on C910, the -59.4% ADP improvement on this unit is attributable to test-time RL on top of the off-the-shelf backbone. The released artifact ships the SFT configuration and merge script so reviewers can re-run the warm-up under any policy of choice.

H Prompt Templates

System prompt. The system prompt is fixed for all problems:

```
You are an expert Verilog RTL designer.
When reasoning, use <think>...</think> tags.
Output only Verilog code within ““verilog fences.
```

The templates below are the RTLLM v2.0 main-run prompts in which the PPA product $M = A \cdot D \cdot P$ is shown to the model. In the C910 LZA ablation (where the OpenSTA power column is not collected) the same templates degenerate to ADP ($M = A \cdot D$); we use the generic placeholder “{M}” below to make this dual usage explicit.

Root state user prompt.

```
## Reference Implementation
Below is a known working implementation that synthesizes to
area={A} $\mu\text{m}^2$ , delay={D}ps, power={P} $\mu\text{W}$  (PPA-product={M}).
Your task is to produce a functionally correct implementation
with lower PPA-product (Area  $\times$  Delay  $\times$  Power).
““verilog
{reference_code}
““

## Design Specification
```

```

{specification}
Write a complete Verilog module with PPA-product lower than {M}.
Output only Verilog code within ““verilog fences.

```

Non-root state user prompt. The non-root prompt appends the following block after the reference and specification:

```

## Previous Attempt
““verilog
{parent_code}
““

## Feedback from Previous Attempt
- Syntax: PASS
- Functional Test: PASS
- Synthesis: area={A} $\mu\text{m}^2$ , delay={D}ps, power={P} $\mu\text{W}$ , PPA-product={M}
Previous PPA-product: {prev_M} -> current: {M} (improved by { $\Delta$ })
You are iteratively optimizing PPA-product (lower is better).
Produce a design with PPA-product lower than {M}.

```

I Entropic Adaptive Beta: Implementation Detail

Stage-1 syntax score. On iverilog failure the syntax reward is $r_{\text{syn}} = 1/(1 + n_{\text{err}})$, additionally multiplied by 0.3 when the log contains a port-binding keyword (port, unknown module, not a module), and falling back to 0.5 when the log cannot be parsed.

Binary search for β^* . The binary search for β^* operates on $[10^{-6}, 10^6]$ with 64 iterations at the current step’s KL budget δ_t . TTT-Discover [Yuksekgonul et al., 2026] sets $\delta_t \equiv \ln 2$ as a constant; we report this as the *fixed* baseline in the KL-budget ablation (Table 3). RTL-Discover replaces the constant with the adaptive controller of Section 3.4; its hyperparameters are listed in Table 9. Intuitively, the constant $\ln 2$ enforces that the group’s softmax distribution is no more concentrated than a Bernoulli(0.5) distribution, preventing the policy gradient from collapsing to a single rollout even when reward differences are large; the adaptive controller relaxes this hard cap and instead modulates δ between $0.25 \ln 2$ and $4 \ln 2$ in response to the four EMA signals described in Section 3.4.

Signals and EMA update. At step t , given the batch of G groups produced by δ_{t-1} , the controller measures four scalar signals: (i) the average policy-vs-reference KL KL_{ref} , (ii) the effective number of distinct rollouts averaged across groups, $\text{eff-n} = \frac{1}{G} \sum_{g=1}^G (\sum_i q_{g,i}^2)^{-1}$, (iii) the fraction of groups with degenerate (constant) reward, const-frac , and (iv) the binary-search saturation rate $\beta_{\text{max-rate}}$ (the fraction of groups whose β^* hits the search bound 10^6). Each signal is smoothed by a single EMA with mixing $\alpha = 0.30$:

$$\bar{x}_t = (1 - \alpha) \bar{x}_{t-1} + \alpha x_t, \quad x \in \{\text{KL}_{\text{ref}}, \text{eff-n}, \text{const-frac}, \beta_{\text{max-rate}}\}. \quad (8)$$

A separate slower EMA with $\alpha_r = 0.10$ tracks the running peak reward \bar{r}_t used by the stagnation counter N_{noimp} , which is incremented when the batch maximum fails to exceed \bar{r}_{t-1} by at least $\Delta r_{\text{min}} = 0.02$ and reset to 0 whenever a new peak is observed.

Priority ladder. For the first $T_{\text{warm}} = 20$ steps only the KL brake (P1) is active, with $\delta_t \equiv \delta_0$ otherwise. Past warm-up, the ladder evaluates P1–P4 in order and applies the assignment of the *first* rule whose guard holds; if none holds, $\delta_t \leftarrow \delta_{t-1}$ (**hold**).

$$\text{(P1) KL brake: } \overline{\text{KL}_{\text{ref}}}_t > \tau_{\text{KL}} \Rightarrow \delta_t \leftarrow \delta_0, \quad (9)$$

$$\text{(P2) winner-take-all: } \overline{\beta_{\text{max-rate}}}_t > \tau_{\beta} \wedge \overline{\text{eff-n}}_t < \tau_n^{\text{wta}} \Rightarrow \delta_t \leftarrow \max(\rho_- \delta_{t-1}, \delta_{\text{min}}), \quad (10)$$

$$\text{(P3) stagnation: } N_{\text{noimp}} \geq T_{\text{stag}} \wedge \overline{\text{const-frac}}_t < \tau_{\text{const}} \wedge \overline{\text{eff-n}}_t < \tau_n^{\text{stag}} \Rightarrow \delta_t \leftarrow \max(\rho_- \delta_{t-1}, \delta_{\text{min}}), \quad (11)$$

$$\text{(P4) over-exploring: } \overline{\text{eff-n}}_t > \tau_n \wedge \overline{\text{const-frac}}_t < \tau_{\text{const}}^{\text{lo}} \wedge N_{\text{noimp}} < T_{\text{plat}} \Rightarrow \delta_t \leftarrow \min(\rho_+ \delta_{t-1}, \delta_{\text{max}}). \quad (12)$$

The *eff-n* joint gates on P2 and P3 (τ_n^{wta} , τ_n^{stag}) are essential: they prevent the controller from shrinking δ when group weights are already near uniform (a flat-reward regime that would collapse

the advantages to zero on further shrinkage), and instead require that the rule that fires acts on a genuinely concentrated group.

Table 4: Per-design ratio on RTLLM v2.0 (lower is better; bold = best per row; “-” = method failed to produce compilable RTL). All four methods report the PPA-product ratio $A \cdot D \cdot P$ against the same v2.0 reference; Evolve / VeriAgent / REvolution numbers are taken from Ping et al. [2026], Table 3 (GPT-4o-mini).

Design	ref M	Evolve	VeriAgent	REvolution	TTT-RTL
JC_counter	10180.4	1.000	1.000	1.000	1.000
LFSR	93.5	1.140	1.140	1.140	1.000
LIFObuffer	28866.5	1.000	0.770	0.770	0.632
RAM	63406.1	1.083	1.026	1.026	1.036
ROM	46.3	1.000	1.000	0.964	1.000
accu	82040.8	1.000	0.904	0.885	0.760
adder_16bit	3513.1	1.000	0.955	0.955	0.872
adder_32bit	25037.3	0.967	0.939	0.967	0.235
adder_8bit	440.0	1.152	1.152	1.152	0.014
adder_bcd	484.6	0.638	0.617	0.638	0.943
adder_pipe_64bit	6109235.7	0.423	0.423	0.423	0.094
alu	3192539.6	0.375	0.348	0.321	0.241
asyn_fifo	580752.5	-	-	-	-
barrel_shifter	94.4	1.127	1.127	1.127	0.840
calendar	9374.5	0.953	0.840	0.953	0.548
comparator_3bit	10.2	0.664	0.600	0.664	0.454
comparator_4bit	26.9	0.621	0.586	0.621	0.234
counter_12	824.7	1.000	1.000	1.000	0.940
div_16bit	9401995.7	1.089	1.045	1.089	0.510
edge_detect	40.5	1.000	0.904	0.904	0.086
fixed_point_adder	233273.1	0.752	0.752	1.000	0.062
fixed_point_subtractor	354996.9	0.888	0.824	0.888	0.201
float_multi	914343626.2	0.453	0.453	0.453	0.129
freq_div	4986.7	0.561	0.526	0.561	0.417
freq_divbyeven	290.5	1.574	-	-	0.607
freq_divbyfrac	388.2	-	-	-	0.561
freq_divbyodd	2347.5	-	-	-	0.425
fsm	429.1	0.476	0.297	0.476	0.011
instr_reg	2415.7	1.000	1.000	1.000	0.143
multi_16bit	2354913.0	0.342	0.342	0.342	0.335
multi_8bit	725109.1	1.000	0.771	0.153	0.311
multi_booth_8bit	196035.4	0.989	0.918	0.918	0.691
multi_pipe_4bit	11025.1	1.000	0.884	0.734	0.750
multi_pipe_8bit	584498.4	1.319	1.000	1.000	0.149
parallel2serial	450.8	1.000	0.965	0.771	0.726
pe	224095126.1	1.000	1.000	0.986	0.996
pulse_detect	153.2	1.000	0.727	0.075	0.174
radix2_div	88514.0	0.973	-	0.973	0.011
right_shifter	108.5	1.000	1.000	1.000	1.000
ring_counter	263.1	1.000	1.000	1.000	0.425
sequence_detector	211.0	1.040	1.040	1.000	0.041
serial2parallel	14019.8	1.027	1.000	1.000	0.782
signal_generator	678.1	0.906	0.894	0.738	0.705
square_wave	12354.9	1.066	1.000	0.954	0.108
sub_64bit	238797.5	0.995	0.899	0.890	0.885
synchronizer	671.8	1.000	0.847	0.706	1.000
traffic_light	32088.5	1.000	1.000	1.000	0.561
up_down_counter	101304.7	1.000	1.000	0.584	0.878
width_8to16	14891.7	0.960	1.000	0.960	0.253
GeoMean (common, $N=44$)	-	0.872	0.813	0.739	0.349
#Best / 44	-	0.5	2.0	8.0	33.5

Table 5: Representative per-design comparison of the v2.0 reference RTL under our local flow vs. the published numbers [Ping et al., 2026]. Area in μm^2 , delay in ns, power in μW ; the Δ columns are signed relative error (ours – pub)/pub. Area and delay are closely matched on the vast majority of designs; absolute power shows larger discrepancies driven by OpenSTA activity / reporting assumptions, which is the reason we only report ratios against the shared reference in the main comparison. Two outlier-style cases (RAM and `asyn_fifo`, where Yosys infers different array / synchronizer structures across flows) are included for completeness.

Design	A_{pub}	A_{ours}	ΔA	D_{pub}	D_{ours}	ΔD	P_{pub}	P_{ours}	ΔP
comparator_3bit	12.0	12.0	+0.0%	0.15	0.16	+6.7%	5.7	4.7	-18.3%
adder_8bit	48.9	48.9	+0.0%	0.31	0.34	+9.7%	29.0	16.8	-42.1%
calendar	164.1	164.9	+0.5%	0.42	0.47	+11.9%	136.0	105.0	-22.8%
adder_16bit	96.8	94.7	-2.2%	0.59	0.67	+13.6%	61.5	40.4	-34.3%
adder_32bit	208.5	211.2	+1.3%	0.87	0.91	+4.6%	138.0	85.1	-38.3%
alu	1953.0	1967.1	+0.7%	1.93	2.10	+8.8%	847.0	688.0	-18.8%
multi_16bit	951.5	933.9	-1.8%	1.98	2.19	+10.6%	1250.0	796.0	-36.3%
adder_pipe_64bit	2529.4	2523.5	-0.2%	0.83	0.90	+8.4%	2910.0	1920.0	-34.0%
pe	3649.5	3640.2	-0.3%	1.72	1.91	+11.0%	35700.0	1400.0	-96.1%
<i>Outlier-style cases (different inferred structure across flows)</i>									
RAM	474.8	633.9	+33.5%	0.22	0.32	+45.5%	607.0	479.0	-21.1%
asyn_fifo	1099.9	1341.7	+22.0%	0.33	0.87	+163.6%	1600.0	1140.0	-28.7%

Table 6: Aggregate flow-sanity statistics over the RTLLM v2.0 designs that synthesize cleanly under both flows. The *Area* row covers all 47 designs that complete area synthesis under both flows; the *Delay* and *Power* rows are restricted to the 43-design subset for which both flows also produce a valid OpenSTA timing report (designs where one flow returns a delay-floor or missing-power report are excluded from those two rows only). Error is signed relative error of our local measurement against the published value; *within-X%* counts designs whose absolute relative error is at most X . The takeaway is that the PPA product’s area and delay components are tightly matched, and the residual cross-flow discrepancy lives almost entirely in absolute power—which the main-result protocol absorbs by reporting only ratios against the shared v2.0 reference.

Component	median err	mean err	within 5%	within 15%
Area	0.6%	6.9%	36/47	43/47
Delay	8.2%	13.4%	19/43	39/43
Power	31.3%	35.8%	4/43	13/43

Table 7: Paired multi-seed comparison on `ct_vfmau_lza_simd_half` (sky130, $n = 4$ adaptive vs. 4 fixed, 100 RL steps each). Mean \pm std across seeds; p -values are paired t -test. No metric reaches $p < 0.05$.

Metric	Direction	adaptive	fixed $\delta = \ln 2$	Δ	paired p
<code>best_reward_ever</code>	↑	21.96 \pm 0.56	21.30 \pm 1.48	+0.67	0.32
<code>end_reward_last20</code>	↑	19.01 \pm 1.60	19.44 \pm 2.00	-0.43	0.57
<code>step_to_score \geq 20</code>	↓	44.5 \pm 33.3	69.5 \pm 77.7	-25.0	0.42
<code>const_group_frac_last20</code>	↓	0.46 \pm 0.18	0.52 \pm 0.09	-0.06	0.58

Table 8: TTT-RTL hyperparameter configuration used in all experiments.

Hyperparameter	Value
Base model	RTLLM v2.0: Qwen3-8B + ttt-rtl-sft step 18 (Section G); C910 LZA: raw Qwen3-8B (no SFT)
Gradient steps per problem	100
Batch size (parent states)	4
Rollouts per prompt (n)	4 (RTLLM v2.0 main runs) / 8 (C910 LZA ablations)
PUCT exploration coefficient (c)	1.0
State pool size (C_{\max})	500
Top- k children per parent	2
Reward weight ω_{syn}	0.1
Reward weight ω_{func}	1.0
Reward weight ω_{ppa}	10.0
KL budget δ_t for β^* search	RTLLM v2.0: fixed $\delta = \ln 2$ (TTT-Discover canonical); C910 LZA: per-row, see Table 3 (incl. adaptive controller of Table 9, range $[0.25 \ln 2, 4 \ln 2]$)
Technology library	Nangate 45 nm (RTLLM v2.0) / Sky130 HD (C910 LZA)
Synthesis tool	Yosys
Functional simulation	iverilog / vvp
Training framework	ver1 [Sheng et al., 2024]

Table 9: Hyperparameters of the adaptive KL-budget controller (Section 3.4). All values are held fixed across all problems and PDKs reported in this paper. Symbols match the priority-ladder description in Section 3.4.

Symbol	Description	Value
δ_0	Init / KL-brake reset value	$\ln 2 \approx 0.693$
δ_{\min}	Lower bound of δ_t	$0.25 \ln 2 \approx 0.173$
δ_{\max}	Upper bound of δ_t	$4 \ln 2 \approx 2.773$
ρ_-	Shrink factor (P2, P3)	0.85
ρ_+	Grow factor (P4)	1.20
α	EMA mixing for KL / eff- n / const-frac / β -rate	0.30
α_r	EMA mixing for reward peak tracking	0.10
τ_{KL}	P1 KL-brake threshold	0.40
τ_β	P2 winner-take-all β -rate threshold	0.60
τ_n^{wta}	P2 eff- n joint gate (sharp groups only)	3.5
T_{stag}	P3 stagnation steps	15
Δr_{\min}	P3 minimum relative improvement	0.02
τ_{const}	P3 const-frac guard (signal exists)	0.70
τ_n^{stag}	P3 eff- n joint gate (sharp groups only)	4.0
τ_n	P4 effective- n threshold	5.5
$\tau_{\text{const}}^{\text{lo}}$	P4 const-frac threshold	0.30
T_{plat}	P4 plateau guard (steps)	5
T_{warm}	Warm-up steps (P1 only)	20

NeurIPS Paper Checklist

1. Claims

Question: Do the main claims made in the abstract and introduction accurately reflect the paper’s contributions and scope?

Answer: [Yes]

Justification: The abstract and introduction state three contributions: (i) a per-design test-time training framework that closes the LLM-EDA loop (Section 3), (ii) external comparison on RTLLM v2.0 reporting a 65.1% geomean PPA-product reduction vs. the v2.0 reference, against 26.1% for the strongest published baseline (Table 1, Section 4.2), and (iii) an industrial C910 LZA case study with a 59.4% ADP reduction and component ablations (Table 3, Section 4.3). The adaptive KL-budget controller is framed as a robustness/task-responsiveness observation rather than a peak-performance win, matching the multi-seed evidence in Section D.

2. Limitations

Question: Does the paper discuss the limitations of the work performed by the authors?

Answer: [Yes]

Justification: **(L1) Single-seed main results.** RTLLM v2.0 and the C910 main-table results are single-seed (matching the published agent baselines, none of which report seed variance); a four-seed paired replication on LZA `simd_half` and a single-seed case study on `ct_vfdsu_fadd_close_s0_d` (Section D) confirm direction and a $\sim 2.6\times$ seed-wise variance reduction but do not reach $p < 0.05$ at $n = 4$, so per-row gaps in Table 3 should be read as ranking evidence rather than tight effect sizes. **(L2) Simulation-only correctness.** Designs are validated against the RTLLM testbench, not formal equivalence; a Yosys eqy check is the natural next step, as is timing-accurate synthesis (OpenROAD [Ajayi et al., 2019] or commercial flows) for more reliable PPA estimates. **(L3) Internal ablation of the controller.** We do not yet report a leave-one-rule-out study of P1–P4 within the adaptive controller, so we cannot claim which rule drives the gain. Section D additionally documents the controller’s negative results: no metric reaches $p < 0.05$ at $n = 4$ on LZA, the fadd δ raise post-dates the breakthrough, and the +0.67 peak gap lies inside the development spread of 15.6–25.7 best-so-far reward observed across development repeats of adaptive- δ + PUCT on the C910 unit.

3. Theory assumptions and proofs

Question: For each theoretical result, does the paper provide the full set of assumptions and a complete (and correct) proof?

Answer: [N/A]

Justification: The paper does not prove new theorems. Section 3 reuses the entropic policy-gradient objective and binary-search β^* from TTT-Discover [Yuksekgonul et al., 2026] and adds an empirical control rule (Section 3.7); we do not claim convergence or optimality results.

4. Experimental result reproducibility

Question: Does the paper fully disclose all the information needed to reproduce the main experimental results of the paper to the extent that it affects the main claims and/or conclusions of the paper?

Answer: [Yes]

Justification: Section 4 and Section F specify the base model (RTLLM v2.0: Qwen3-8B + `ttt-rtl-sft` step 18; C910 LZA: raw Qwen3-8B with no SFT), training framework (`ver1`), 100-step budget, $B = 4$ parents, $n \in \{4, 8\}$ rollouts, PUCT $c = 1.0$, pool cap $C_{\max} = 500$, reward weights (Equation (3)), KL-budget controller hyperparameters (Table 9), PDKs (Nangate 45 nm, Sky130 HD), tools (Yosys, OpenSTA, iverilog), seed (42), and prompt templates (Section H). The artifact (to be released on GitHub) ships per-rollout logs, all generated Verilog, synthesis scripts, liberty-file manifests, and machine-readable result tables; re-evaluating any reported ratio from the released Verilog requires no retraining.

5. Open access to data and code

Question: Does the paper provide open access to the data, code, and instructions needed to faithfully reproduce the main experimental results, as described in supplemental material?

Answer: [Yes]

Justification: All datasets and PDKs are public: RTLLM v2.0 [Lu et al., 2024, Liu et al.,

2025], the open-source XuanTie C910 RTL [Chen et al., 2020], Nangate 45 nm and Sky130. The artifact (to be released on GitHub under Apache 2.0) contains synthesis scripts, generated Verilog, prompts, and result CSVs; the training code and SFT checkpoint will be released alongside.

6. **Experimental setting/details**

Question: Does the paper specify all the training and test details (e.g., data splits, hyperparameters, how they were chosen, type of optimizer, etc.) necessary to understand the results?

Answer: [Yes]

Justification: Per-run hyperparameters are in Section 4 (training config, sampling budget, baselines, synthesis flow, PDK choice) and Section F and Table 9. We also disclose the hyperparameter selection protocol: TTT-Discover defaults are inherited unmodified except for the adaptive KL-budget controller, whose thresholds were fixed once on the C910 LZA pilot and held constant across all 49 RTLLM v2.0 designs and the second C910 unit (Section 3.7, Section D).

7. **Experiment statistical significance**

Question: Does the paper report error bars suitably and correctly defined or other appropriate information about the statistical significance of the experiments?

Answer: [Yes]

Justification: The main RTLLM v2.0 and C910 main-table numbers are single-seed, matching all three published agent baselines (none of EvoLVE / VeriAgent / REvolution report seed variance), and we say so explicitly in Section 4 and Table 3 (“All rows are single-seed”). For the adaptive vs. fixed δ contrast, Section D reports a four-seed paired replication on LZA `simd_half` with mean \pm std and paired t -test p -values for four metrics (Table 7), an exhaustive enumeration over all 24 adaptive-to-fixed pairings, leave-one-out checks, and a single-seed second-task replication on `fadd_close_s0_d`. The negative-significance results are reported alongside the positive variance-reduction result.

8. **Experiments compute resources**

Question: For each experiment, does the paper provide sufficient information on the computer resources (type of compute workers, memory, time of execution) needed to reproduce the experiments?

Answer: [Yes]

Justification: All experiments use A800 GPUs. RTLLM v2.0: each of the 49 designs runs on 2 nodes \times 4 A800 GPUs (8 GPUs total), wall-clock \sim 2 h per design (\sim 16 GPU-h per design); the full 49-design sweep is \sim 780 GPU-h. C910 LZA ablations: each row runs on 1 node \times 8 A800 GPUs, wall-clock \sim 4.5 h per row (\sim 36 GPU-h per row); the 8 ablation rows in Table 3 total \sim 320 GPU-h. The seed and replication protocol is in Section 4 (“Compute and seed protocol”).

9. **Code of ethics**

Question: Does the research conducted in the paper conform, in every respect, with the NeurIPS Code of Ethics?

Answer: [Yes]

Justification: The work uses publicly released model weights (Qwen3-8B), public benchmarks (RTLLM v2.0), and the open-source XuanTie C910 RTL under their respective permissive licenses. No human subjects, no crowdsourcing, no scraped or private data are involved. The synthesized RTL is hardware-design output, not personal data.

10. **Broader impacts**

Question: Does the paper discuss both potential positive societal impacts and negative societal impacts of the work performed?

Answer: [Yes]

Justification: TTT-RTL targets PPA reduction in fixed-function hardware modules, which can reduce energy and silicon area for deployed designs. Negative impacts are limited: the framework requires both an LLM and a full EDA flow, so it does not lower the barrier to malicious hardware generation beyond what is already achievable with standard EDA tools. We do not foresee dual-use risk that would warrant a release-time gating mechanism beyond the standard model card.

11. **Safeguards**

Question: Does the paper describe safeguards that have been put in place for responsible

release of data or models with a high risk for misuse (e.g., pretrained language models, image generators, or scraped datasets)?

Answer: [N/A]

Justification: We release fine-tuned Verilog-domain weights of an existing public base model (Qwen3-8B) plus per-design rollout logs and synthesis scripts. The artifact does not contain scraped data, pretrained generative models for natural-language or image content, or any content with elevated misuse risk relative to the base model.

12. Licenses for existing assets

Question: Are the creators or original owners of assets (e.g., code, data, models), used in the paper, properly credited and are the license and terms of use explicitly mentioned and properly respected?

Answer: [Yes]

Justification: All third-party assets are cited in-text and respected in license: Qwen3-8B [Yang et al., 2025] (Apache 2.0), ver1 [Sheng et al., 2024] (Apache 2.0), Yosys [Wolf and Glaser, 2013] (ISC), OpenSTA (GPLv3), iverilog (GPLv2), Nangate Open Cell Library 45 nm (Apache-style), Sky130 PDK (Apache 2.0), RTLLM v2.0 [Lu et al., 2024, Liu et al., 2025] (MIT), the XuanTie C910 RTL [Chen et al., 2020] (Apache 2.0), and baseline numbers from Ping et al. [2026] (released under MIT). Per-asset versions are listed in Sections 4 and F.

13. New assets

Question: Are new assets introduced in the paper well documented and is the documentation provided alongside the assets?

Answer: [Yes]

Justification: New assets are: (a) the TTT-RTL training code, (b) the `ttt-rtl-sft` SFT checkpoint, (c) generated Verilog for all $49 \times 4 = 196$ method \times design rollout pools, and (d) the `reference_ppa_measured.csv` flow-sanity table (Section B). The artifact contains a top-level README with the directory layout, run instructions, license (Apache 2.0), and per-design provenance metadata. Section F doubles as a model card for the SFT checkpoint.

14. Crowdsourcing and research with human subjects

Question: For crowdsourcing experiments and research with human subjects, does the paper include the full text of instructions given to participants and screenshots, if applicable, as well as details about compensation (if any)?

Answer: [N/A]

Justification: No crowdsourcing or human-subjects studies were conducted. All evaluation signals come from automated EDA tools (Yosys, OpenSTA, iverilog) on public Verilog inputs.

15. Institutional review board (IRB) approvals or equivalent for research with human subjects

Question: Does the paper describe potential risks incurred by study participants, whether such risks were disclosed to the subjects, and whether Institutional Review Board (IRB) approvals (or an equivalent approval/review based on the requirements of your country or institution) were obtained?

Answer: [N/A]

Justification: No human-subjects research was performed; IRB review does not apply.

16. Declaration of LLM usage

Question: Does the paper describe the usage of LLMs if it is an important, original, or non-standard component of the core method development in this research?

Answer: [Yes]

Justification: An LLM is the central object of study—the policy that TTT-RTL fine-tunes per design. The base model (Qwen3-8B), the SFT corpus (`ttt-rtl-sft`, step 18), the training framework (`ver1`), the prompt templates (Section H), and all training-time hyperparameters (Tables 8 and 9) are documented in Section 4 and the appendix. LLMs were not used as a tool for paper writing or experiment design beyond standard authorial assistance, and any such use does not affect the reported methodology, results, or originality.